

The Ndc80/HEC1 complex is a contact point for kinetochore-microtubule attachment

Ronnie R Wei^{1,2}, Jawdat Al-Bassam¹ & Stephen C Harrison²

Kinetochores are multicomponent assemblies that connect chromosomal centromeres to mitotic-spindle microtubules. The Ndc80 complex is an essential core element of kinetochores, conserved from yeast to humans. It is a rod-like assembly of four proteins—Ndc80p (HEC1 in humans), Nuf2p, Spc24p and Spc25p. We describe here the crystal structure of the most conserved region of HEC1, which lies at one end of the rod and near the N terminus of the polypeptide chain. It folds into a calponin-homology domain, resembling the microtubule-binding domain of the plus-end-associated protein EB1. We show that an Ndc80p-Nuf2p heterodimer binds microtubules *in vitro*. The less conserved, N-terminal segment of Ndc80p contributes to the interaction and may be a crucial regulatory element. We propose that the Ndc80 complex forms a direct link between kinetochore core components and spindle microtubules.

Kinetochores assemble on centromeric DNA and attach to spindle microtubules during cell division. The attachments are stable through phases of microtubule polymerization and depolymerization, and they generate forces involved in chromosome movement during metaphase and anaphase¹. Kinetochores also regulate cell-cycle progression at the metaphase-to-anaphase transition through the spindle-assembly checkpoint². These crucial activities require concerted interactions among the large number of proteins and protein complexes now known to participate.

The simplest kinetochores, those of *Saccharomyces cerevisiae*, contain 60 or more distinct subunits, many in multiple copies, assembled into at least 14 multiprotein complexes^{3,4}. In higher eukaryotes, electron microscopy of kinetochores reveals a trilaminar structure, with an electron-dense inner domain containing centromeric heterochromatin, a less dense middle domain, and an outer domain containing microtubule-binding activities⁵. Short, 125-base-pair point centromeres are sufficient for accurate chromosome segregation in budding yeast, whereas the regional centromeres found in human cells span megabases of DNA, and those in fission yeast 40 kilobases or more^{6–8}. Kinetochores in higher eukaryotes bind 30 or more microtubules; those of budding yeast, a single microtubule^{9–11}. Despite these large differences, sequences of kinetochore proteins from various species reveal that many *S. cerevisiae* kinetochore components have been conserved from yeast to humans¹². Among the most conserved are the four proteins of the Ndc80 complex, essential for proper chromosome alignment and segregation during mitosis¹³.

Inactivation of Ndc80 complex proteins in fungi and metazoa causes chromosomes to detach from spindle microtubules. When the Ndc80 complex is depleted, checkpoint proteins such as Mad1p and Mad2p no longer associate with kinetochores or do so at greatly

reduced levels (reviewed in ref. 13). Human Ndc80 (known as HEC1) and human Nuf2 (NUF2) are present at the outer plate as stable components throughout mitosis, in contrast with the more dynamic distribution of motor and checkpoint proteins. They are essential for maintaining the integrity of the outer plate and for establishing stable kinetochore-microtubule attachment and tension¹⁴. In yeast, the Ndc80 complex requires the DNA-binding complex CBF3 for localization at centromeres, and it is in turn essential for stable association of outer kinetochore proteins, including Stu2p, Dam1p, Cin8p in yeast^{15,16} and Zw10 in *Xenopus laevis*¹⁷. Unlike various kinetochore-related, microtubule-associated proteins, such as the DASH–Dam1 complex and EB1 (refs. 18,19), Ndc80 does not require microtubules to participate in kinetochore assembly.

The four components of the Ndc80 complex—Ndc80p, Nuf2p, Spc24p and Spc25p—assemble into a heterotetrameric rod, about 570 Å long, with globular ‘heads’ at either end of an α -helical coiled-coil shaft²⁰. Ndc80p and Nuf2p contribute to one head and to the intervening shaft. In an attached kinetochore, the head domains are likely to point toward the microtubule, as they require Spc24p and Spc25p to join the kinetochore assembly²¹. Spc24p and Spc25p complete the shaft and contribute to the other head, which points toward the centromere. Fluorescence microscopy shows that each kinetochore contains at least five to ten Ndc80 complexes⁴. Thus, the properties of the complex suggest that it is a crucial bridge between microtubules and centromere-proximal structures. Its length is such that it could, in principle, bridge between the outer and inner layers of a trilaminar kinetochore^{20,22}.

We have recently described the crystal and solution structures of the Spc24p–Spc25p globular domains, which fold into a single, globular entity²³. Its structure does not correspond to a previously described

¹Department of Biological Chemistry and Molecular Pharmacology and ²Howard Hughes Medical Institute, Harvard Medical School, 250 Longwood Avenue, Boston, Massachusetts 02115, USA. Correspondence should be addressed to S.C.H. (harrison@crystal.harvard.edu).

Received 27 November; accepted 1 December; published online 31 December 2006; doi:10.1038/nsmb1186

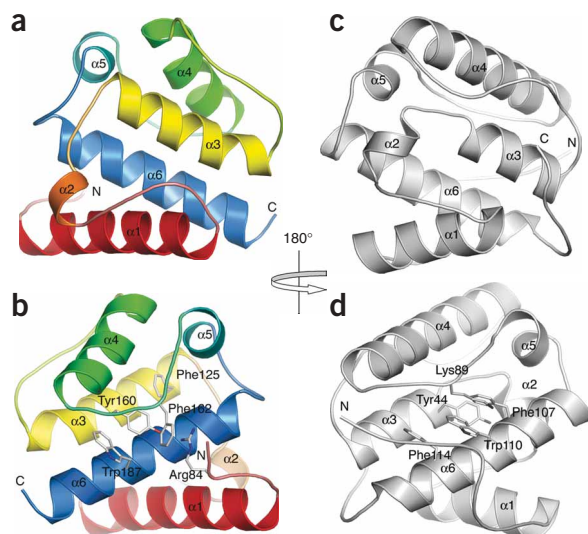


Figure 1 Structure of the HEC1 globular domain, compared with the EB1 microtubule-binding domain. **(a)** Ribbon diagram of HEC1_CH (HEC₈₁₋₁₉₆). **(b)** View from the opposite direction to **a**, showing the potential microtubule-binding site, analogous to that on EB1. Side chains of Arg84, Phe125, Tyr160, Phe162 and Tyr187 are shown as sticks. **(c)** Ribbon diagram of EB1 microtubule-binding domain (PDB 1PA7)²⁴ in the same orientation as HEC1_CH in **a**. **(d)** EB1 microtubule-binding domain, in the same orientation as HEC1_CH in **b**, showing the proposed microtubule-binding site²⁴. The side chains of Lys89 and its surrounding hydrophobic residues are shown as sticks, with O and N in red and blue, respectively. N and C termini are labeled.

interaction module, but it does have a marked cleft, which faces away from the coiled-coil shaft. We have suggested that this cleft is the contact point for a centromere-proximal kinetochore protein. We have now determined the crystal structure of the most conserved region of the HEC1 globular domain (residues 81–196). It belongs to a family of proteins known as calponin-homology (CH) domains, many of which bind cytoskeletal proteins. We have gone on to show that the Ndc80p-Nuf2p globular regions indeed associate with microtubules *in vitro*. Inclusion of the less conserved, N-terminal extension of Ndc80p strengthens the interaction, and we suggest that this extension, a site of phosphorylation by Aurora B kinases (Ipl1p in *S. cerevisiae*), is a functionally important regulatory element.

RESULTS

HEC1/Ndc80p contains a calponin-homology domain

Crystals of HEC₈₁₋₁₉₆, prepared as described in Methods, yielded diffraction data to a Bragg spacing of 1.8 Å. We determined the structure using MAD. The domain has six α -helices (**Fig. 1a,b**), organized in a CH domain fold; we designate it as HEC1_CH in the rest of the text. CH domains are present in many actin-binding proteins and also in the microtubule-binding protein EB1 (ref. 24). By use of the Dali program²⁵, we found that HEC1_CH has closest structural similarity to the first CH repeat of human fimbrin²⁶ (PDB 1AOA; Dali Z-score = 8.4; r.m.s. deviation = 2.7 Å for 99 C α atoms; 4% sequence identity); the N-terminal, microtubule-binding domain (residues 1–126) of EB1 (ref. 24) is also very similar (PDB 1PA7; Z-score = 6.3; r.m.s. deviation = 3.3 Å for 91 C α atoms; 11% sequence identity) (**Fig. 1c,d**). CH domains all have four principal α -helices ($\alpha 1$, $\alpha 3$, $\alpha 4$ and $\alpha 6$), which form a parallel, four-helix bundle. Two or three short, less regular helices ($\alpha 2$ and $\alpha 5$ in HEC1_CH) are minor secondary structure elements. Aliphatic residues from $\alpha 3$ and $\alpha 6$ contribute to the hydrophobic core²⁷ (**Figs. 1** and **2**).

The CH domain is a conserved structural unit with diverse biological functions. Two CH domains in tandem form a high affinity F-actin-binding module in a large number of actin-cross-linking proteins such as α -actinin and fimbrin²⁸. Crystal structures suggest that a compact assembly of the two CH domains is the actin-binding unit, but the details remain to be clarified^{29,30}. The microtubule-binding protein EB1, conserved in all eukaryotes, has a single CH domain^{24,31}. It can bind along the length of microtubules, but it

localizes preferentially to the plus ends of kinetochore-bound microtubules during mitosis as well as to the plus ends of cytoskeletal microtubules during interphase³¹. EB1 binds microtubules as a homodimer, held together by a 40-residue coiled-coil, which connects to the N-terminal CH domain through a flexible linker³². The Ndc80p-Nuf2p heterodimer has a similar quaternary organization, but with a much longer coiled-coil. The likely microtubule-binding site on EB1 maps to the neighborhood of Lys89, on the loop connecting $\alpha 4$ and $\alpha 5$ (L4,5); mutation of this residue to glutamate abolishes microtubule binding²⁴. The side chain of Lys89 is buttressed by aromatic residues on $\alpha 6$, part of the hydrophobic core (**Fig. 1d**)²⁴. The surface of HEC1_CH that corresponds to the proposed microtubule-binding site on EB1 has an exposed hydrophobic cluster, containing conserved aromatic residues in L4,5 and $\alpha 6$ (**Fig. 1b,d** and **Fig. 2**). The N-terminal segment of HEC1_CH traverses one edge of this hydrophobic cluster. It is secured in place by interactions between the side chain of Arg84 and those of Tyr160 and Phe162 in L4,5, augmenting the conserved surface (**Fig. 1b** and **Fig. 2b**). This region is therefore a good candidate for microtubule binding. It is also the most extensive region of conservation on the molecular surface (**Fig. 2a,b**).

The Ndc80 complex interacts directly with microtubules

We carried out a series of microtubule cosedimentation assays with different recombinant constructs of Ndc80/HEC1, to test whether it can indeed interact directly with microtubules. Unlike the monomeric, N-terminal domain of EB1, which cosediments with microtubules²⁴, HEC1_CH alone does not bind microtubules under the conditions we explored (data not shown). We used the *S. cerevisiae* Ndc80 complex, from which we had previously prepared well-characterized fragments, to determine whether an Ndc80p-Nuf2p heterodimer can interact with microtubules. We purified recombinant heads of Ndc80p-Nuf2p, held together through the proximal part of the coiled coil (2NG; see Methods). The Ndc80 chain included a roughly 100-residue, non-conserved, N-terminal segment not present in the crystal structure of HEC1_CH (see next paragraph). The 2NG heterodimer bound taxol-stabilized microtubules, assembled from purified bovine-brain tubulin, with an affinity similar to that of EB1 (**Fig. 3** and **Supplementary Fig. 1** online). There was detectable interaction even at NaCl concentrations as high as 500 mM (data not shown), effectively ruling out a purely nonspecific electrostatic affinity. As the concentration of 2NG increased, binding saturated at one or two heterodimers of 2NG per heterodimer of tubulin (**Fig. 3**).

Ndc80 homologs have an extended N-terminal segment that is highly variable in length (~110 residues for *S. cerevisiae* and 80 for human, respectively) and sequence, but consistently rich in positive charge. Although it was not included in our crystallization construct, owing to its presumed flexibility, this extension would project along the proposed microtubule-binding surface, like the extended N-terminal fragment present in the EB1 structure (**Fig. 1b,d**). We

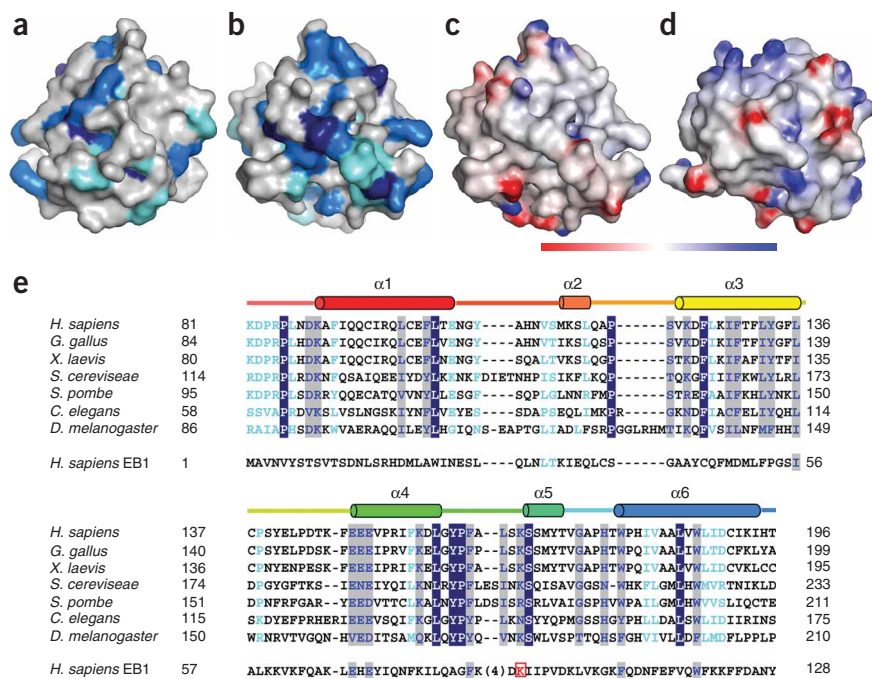


Figure 2 Surface properties of HEC1_CH. (a,b) Surface representations of HEC1_CH in the orientations of **Figure 1a,b**, respectively, colored by degree of conservation (dark blue, most conserved; white, least conserved), showing that the potential microtubule-binding surface is conserved across species. (c,d) Surface representations showing electrostatic potential of HEC1_CH and EB1 microtubule-binding domain, in the orientations of **Figure 1b,d**, respectively. Red to blue, $-15 k_B T$ to $+15 k_B T$, as calculated by Delphi⁴⁹. (e) Multiple sequence alignment for Ndc80/HEC1 and EB1 CH domain (bottom), generated with CLUSTAL W⁵⁰. Secondary structural elements derived from the crystal structure are colored as in **Figure 1a**. Number of initial residue for each homolog is shown after species name. Residues are colored by degree of conservation: white letters on dark blue background, identical; blue on blue-gray, strongly conserved; light blue on white, weakly conserved. Lys89 of EB1, which is required for microtubule binding, is boxed in red.

prepared a heterodimer of *S. cerevisiae* Ndc80p-Nuf2p heads with the first 114 residues of Ndc80p deleted (2NGΔN) and found that this species also binds microtubules, but with approximately seven- to ten-fold lower affinity than does intact 2NG (**Fig. 3b**). The 114-residue segment expressed alone showed no detectable binding *in vitro* (**Supplementary Fig. 2** online). Full-length Ndc80 complex also bound microtubules, but we were unable to determine a K_d , owing to aggregation of the complex at high concentration. The Ndc80p fragment containing both the N-terminal segment and the CH domain was insoluble, even at low concentration. The Spc24p-

Spc25p globular domain did not cosediment with microtubules (data not shown).

We further demonstrated the microtubule-binding activity of 2NG and 2NGΔN by negative-stain electron microscopy (**Fig. 3c**). At a concentration of 2NG at which microtubules were nearly saturated in the cosedimentation assay, there was a dense halo of stain-exclusion along the microtubule walls. Individual 2NG complexes are too small to be discerned by this method. At the same concentration of 2NGΔN, microtubules were less than 25% saturated in the cosedimentation assay, and the stain-excluding halo was correspondingly weaker.

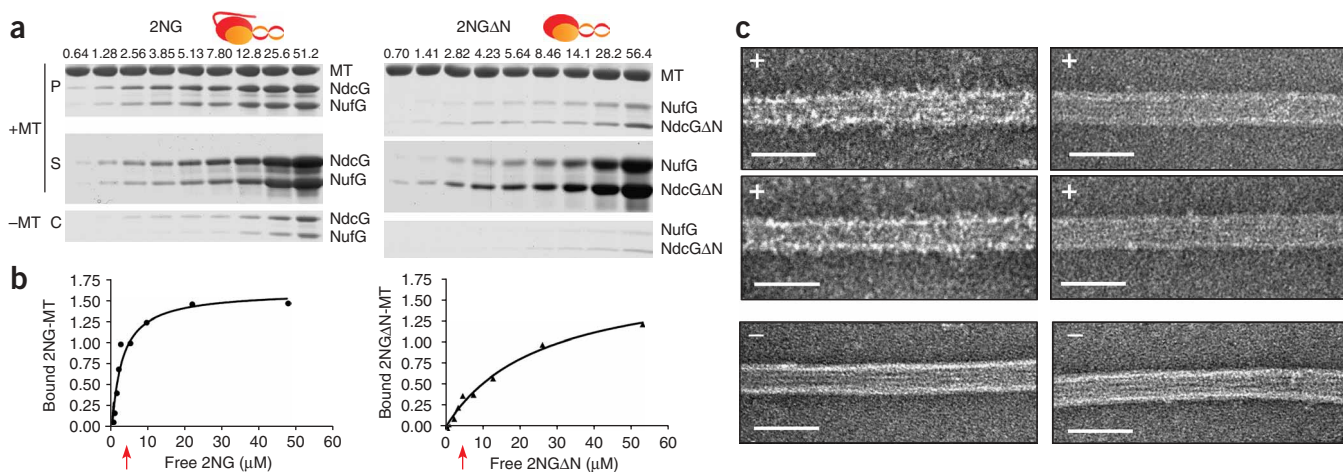


Figure 3 Microtubule binding by 2NG and 2NGΔN. Drawings at top illustrate the parts of the Ndc80 complex present in the respective constructs. (a) Analysis by SDS-PAGE of cosedimentation. Concentration of input protein in each sample (μM) is shown at top of lane. Upper gel (P) shows protein in pellets sedimented in the presence of microtubules; middle panel (S) shows unbound protein in supernatant in the presence of microtubules; lower panel (C) is control showing background protein sedimentation without microtubules. (b) Protein bound to microtubule (normalized as moles per mole of tubulin heterodimer) plotted against free protein concentration. Dissociation constants derived from these curves, \pm s.e.m.: 2NG, $K_d = 2.8 \pm 0.7 \mu\text{M}$; 2NGΔN, $K_d = 25.5 \pm 4.9 \mu\text{M}$. Red arrows indicate concentrations used for EM. (c) Negative-stain EM of microtubules mixed with 2NG (left column, +) and 2NGΔN (right column, +). At concentration shown by arrow in **b**, 2NG binds and forms a halo of stain exclusion along the microtubule wall. Halo is much less pronounced in samples with equal amounts of 2NGΔN. Microtubules stained in the absence of added protein are shown at bottom (-). Scale bars, 500 Å.

DISCUSSION

Our structural and biochemical results show that the heads of Ndc80p/HEC1 and Nuf2p, joined as a heterodimer by a distal coiled-coil, together form a microtubule-binding unit. The general resemblance to homodimeric EB1 is noteworthy, although lack of the Nuf2p globular-domain structure makes more detailed discussion of their relationship premature, and we do not yet know whether Nuf2p contributes directly to microtubule binding or merely to the stability of the Ndc80p fragment we used in the binding experiments. The variable, N-terminal segment of Ndc80p is neither sufficient nor essential for microtubule binding, but when present, it enhances affinity. The N-terminal segment connects to the CH domain through residues adjacent to the proposed microtubule-binding surface (Fig. 1b). It is therefore suitably positioned to regulate the Ndc80 CH domain–microtubule interaction.

The Aurora B (or Ipl1p) kinase is thought to monitor chromosome bipolar attachment by sensing the tension generated when kinetochores of cohesin-linked chromosomes are drawn toward opposite poles^{33,34}. Several Aurora B phosphorylation sites map to the non-conserved, nonglobular, N-terminal segment of Ndc80/HEC1 (Ser100 of *S. cerevisiae* Ndc80p; Ser5, Ser15, Ser55, Ser62, Ser69 and Thr49 of HEC1)^{35–37}. Cells expressing mutants of HEC1 that cannot be phosphorylated at these sites show hyperstretching of centromeres, an indication of heightened tension across the kinetochore³⁷. These *in vivo* experiments imply that the N-terminal segment of Ndc80/HEC1 can affect the stability of kinetochore–microtubule attachment, just as it modulates binding of heterodimeric Ndc80p–Nuf2p to microtubules *in vitro* (Fig. 3). A conserved characteristic of this segment is its strong net positive charge, a property known to favor microtubule association. We suggest that when lack of tension activates or recruits Ipl1p/Aurora B, phosphorylation of the Ndc80 N-terminal segment reduces its net charge, weakens the microtubule–kinetochore contact and enhances the detachment rate. This suggestion is consistent with a report, published while the present paper was under review, showing that the *Caenorhabditis elegans* homolog of Ndc80p–Nuf2p binds microtubules *in vitro* and that addition of Ipl1p and ATP weakens the contact³⁸. That report includes evidence that KNL-1/Spc105p, which also binds microtubules, enhances the Ndc80–microtubule interaction, but only in the presence of the heterotetrameric MIND complex.

The association of kinetochores with microtubules withstands multiple cycles of microtubule polymerization and depolymerization and sustains substantial tension. A single Ndc80–microtubule contact would not have these properties, but multiple, moderate-affinity contacts between the five to ten copies of the Ndc80 complex in a budding-yeast kinetochore, and the single microtubule to which it attaches, could provide the required combination of plasticity and strength. We also note that there may be multiple modes of kinetochore–microtubule interaction at different stages during metaphase and anaphase. The initial encounter between chromosomes and spindle microtubules is thought to

involve association along the side of a microtubule, with stable end binding achieved later³⁹. Thus, Ndc80 probably provides only one component of the kinetochore–microtubule interface, to which other contributors seem to include KNL/Spc105p and (in yeast) the DASH–Dam1 ring^{40,41}.

METHODS

Sample preparation. Human HEC1_CH (residues 81–196) and full-length human EB1 were amplified from a human complementary DNA library and cloned into pET28a(+) (Novagen) with a cleavable His₆ tag fused to the N terminus of each. The proteins were overexpressed in Rosetta pLyS cells (Novagen) induced by 1 mM IPTG and purified by nickel–nitrilotriacetic acid chromatography (Qiagen) followed by size-exclusion chromatography on an S200 16/60–Sephadex column (GE Healthcare). The selenomethionyl (SeMet) HEC1_CH derivative was expressed in the methionine auxotroph cell line BL834(DE3) (Novagen) and purified in the same way as the native protein. Yeast NdcGp (residues 1–343) and NufGp (residues 1–223), or NdcGAN (residues 114–343) and NufGp, were coexpressed and purified as described²⁰.

Structure determination. Proteins were concentrated to 20 mg ml⁻¹ in 20 mM bis-tris propane (pH 7.6), 250 mM NaCl, 5 mM 2-mercaptoethanol and 10 mM DTT, and crystallized by hanging drop vapor diffusion against a reservoir solution of 0.1 M cacodylate (pH 6.5), 22%–30% (w/v) PEG 8,000 and 0.2 M (NH₄)₂SO₄. Crystals were transferred to a reservoir solution supplemented with 20% (v/v) glycerol before flash-freezing in liquid nitrogen. The native and MAD data were collected at Advanced Light Source beamline 8.2.2 and processed using HKL2000 (ref. 42). Positions of two of the three selenium sites were located using SOLVE⁴³. Density modification and initial model building were done using RESOLVE⁴⁴, which gave a figure of merit of 0.84. Model building with O⁴⁵ and COOT⁴⁶ was iterated with refinement against the native data using REFMAC5 (ref. 47). Data collection and refine-

Table 1 Data collection, phasing and refinement statistics

	Native	SeMet		
Data collection				
Space group	<i>P</i> 2 ₁ 2 ₁ 2 ₁	<i>P</i> 2 ₁ 2 ₁ 2 ₁		
Cell dimensions				
<i>a</i> , <i>b</i> , <i>c</i> (Å)	40.91, 44.71, 69.19	40.91, 44.71, 69.19		
		<i>Peak</i>	<i>Inflection</i>	<i>Remote</i>
Wavelength	0.9199	0.97973	0.97986	0.95370
Resolution (Å)	50.00–1.80	50.00–1.90	50.00–1.90	50.00–1.90
<i>R</i> _{sym} (%)	7.5	7.8	7.4	7.8
<i>I</i> / σ <i>I</i>	26.7 (4.25)	20.7 (2.4)	20.6 (2.3)	19.7 (2.2)
Completeness (%)	100 (100)	99.3 (93.8)	98.8 (90.1)	98.8 (89.4)
Redundancy	7.0 (6.9)	4.5 (3.8)	4.5 (3.6)	4.5 (3.6)
Refinement				
Resolution (Å)	37.4–1.8			
No. reflections	12,129			
<i>R</i> _{work} / <i>R</i> _{free} (%)	19.9 / 23.1			
No. atoms				
Protein	935			
Water	77			
<i>B</i> -factors				
Protein	16.15			
Water	25.6			
R.m.s. deviations				
Bond lengths (Å)	0.015			
Bond angles (°)	1.43			

One native and one SeMet crystal were used to solve the structure. Values in parentheses are for highest-resolution shell.

ment statistics are listed in **Table 1**. Of the residues, 92.9% are in the most favored and 7.1% are in the additionally allowed region of the Ramachandran plot, and none are in disallowed regions.

Microtubule cosedimentation assay. Microtubule polymerization from purified tubulin (Cytoskeleton Inc.) and centrifugation were carried out according to published procedures^{19,48}. Increasing amounts of 2NG, 2NGAN or EB1 were incubated with or without 2.7 μM microtubule in 10 mM HEPES (pH 7.0) and 200 mM NaCl at room temperature for 15 min before being sedimented in a TLA-100 rotor (Beckman Coulter) at 214,000g. for 15 min at 25 °C. Protein pellets were resuspended and analyzed by SDS-PAGE. The amount of protein that cosedimented with microtubules was determined by densitometry (ImageQuant TL, GE Healthcare) of the Coomassie-stained protein bands, after subtracting the background (proteins alone without microtubule). Unbound (free) protein concentration was calculated by subtracting the bound protein concentration from the total protein concentration. The fraction of proteins bound to microtubules was plotted as a function of free protein concentration, and the K_d was determined from the best fit to a single-site binding curve.

Electron microscopy. Microtubules were diluted to 0.2 mg ml⁻¹ and mixed with 5 μM 2NG or 2NGAN for 15 min in the same buffer as for the microtubule cosedimentation assay. A drop of an incubated sample was deposited on a positively glow-discharged, carbon-coated copper mesh grid for 2 s and then immediately blotted and stained with 1% (w/v) uranyl acetate. After staining for 1 min, the grids were blotted and air-dried. 2NG-decorated, 2NGAN-decorated and undecorated microtubule specimens were imaged using a Philips CM120 electron microscope operated at 120 keV. EM images were collected using a Gatan CCD at a nominal magnification of $\times 30,000$.

Accession codes. Protein Data Bank: Coordinates have been deposited with accession code 2IGP.

Note: Supplementary information is available on the Nature Structural & Molecular Biology website.

ACKNOWLEDGMENTS

The authors thank J.J. Miranda for help with the microtubule cosedimentation assay, D. Panne for assistance with X-ray data collection and E. Salmon, J. Deluca, N. Larsen, P.R. Ohi and V. Draviam for critique of the manuscript. We acknowledge the Advanced Light Source at Lawrence Berkeley National Laboratory. J.A.-B. is a recipient of the American Cancer Society postdoctoral fellowship. S.C.H. is an investigator of the Howard Hughes Medical Institute.

AUTHOR CONTRIBUTIONS

R.R.W. contributed to the design and execution of the structure determination of HEC1_CH, the microtubule cosedimentation experiments and manuscript preparation. J.A.-B. and R.R.W. contributed the negative-stain electron microscopy. S.C.H. guided the project and helped prepare the manuscript.

COMPETING INTERESTS STATEMENT

The authors declare that they have no competing financial interests.

Published online at <http://www.nature.com/nsmb/>

Reprints and permissions information is available online at <http://npg.nature.com/reprintsandpermissions/>

- Koshland, D.E., Mitchison, T.J. & Kirschner, M.W. Polewards chromosome movement driven by microtubule depolymerization *in vitro*. *Nature* **331**, 499–504 (1988).
- Cleveland, D.W., Mao, Y. & Sullivan, K.F. Centromeres and kinetochores: from epigenetics to mitotic checkpoint signaling. *Cell* **112**, 407–421 (2003).
- McAinsh, A.D., Tjell, J.D. & Sorger, P.K. Structure, function, and regulation of budding yeast kinetochores. *Annu. Rev. Cell Dev. Biol.* **19**, 519–539 (2003).
- Joglekar, A.P., Bouck, D.C., Molk, J.N., Bloom, K.S. & Salmon, E.D. Molecular architecture of a kinetochore-microtubule attachment site. *Nat. Cell Biol.* **8**, 581–585 (2006).
- Roos, U.P. Light and electron microscopy of rat kangaroo cells in mitosis. II. Kinetochore structure and function. *Chromosoma* **41**, 195–220 (1973).
- Chikashige, Y. *et al.* Composite motifs and repeat symmetry in *S. pombe* centromeres: direct analysis by integration of NotI restriction sites. *Cell* **57**, 739–751 (1989).

- Clarke, L. & Carbon, J. Isolation of the centromere-linked CDC10 gene by complementation in yeast. *Proc. Natl. Acad. Sci. USA* **77**, 2173–2177 (1980).
- Cottarel, G., Shero, J.H., Hieter, P. & Hegemann, J.H. A 125-base-pair CEN6 DNA fragment is sufficient for complete meiotic and mitotic centromere functions in *Saccharomyces cerevisiae*. *Mol. Cell. Biol.* **9**, 3342–3349 (1989).
- Peterson, J.B. & Ris, H. Electron-microscopic study of the spindle and chromosome movement in the yeast *Saccharomyces cerevisiae*. *J. Cell Sci.* **22**, 219–242 (1976).
- McDonald, K.L., O'Toole, E.T., Mastronarde, D.N. & McIntosh, J.R. Kinetochore microtubules in PTK cells. *J. Cell Biol.* **118**, 369–383 (1992).
- Winey, M. *et al.* Three-dimensional ultrastructural analysis of the *Saccharomyces cerevisiae* mitotic spindle. *J. Cell Biol.* **129**, 1601–1615 (1995).
- Meraldi, P., McAinsh, A.D., Rheinbay, E. & Sorger, P.K. Phylogenetic and structural analysis of centromeric DNA and kinetochore proteins. *Genome Biol.* **7**, R23 (2006).
- Kline-Smith, S.L., Sandall, S. & Desai, A. Kinetochore-spindle microtubule interactions during mitosis. *Curr. Opin. Cell Biol.* **17**, 35–46 (2005).
- Deluca, J.G. *et al.* Hec1 and nuf2 are core components of the kinetochore outer plate essential for organizing microtubule attachment sites. *Mol. Biol. Cell* **16**, 519–531 (2005).
- He, X., Rines, D.R., Espelin, C.W. & Sorger, P.K. Molecular analysis of kinetochore-microtubule attachment in budding yeast. *Cell* **106**, 195–206 (2001).
- Janke, C., Ortiz, J., Tanaka, T.U., Lechner, J. & Schiebel, E. Four new subunits of the Dam1-Duo1 complex reveal novel functions in sister kinetochore biorientation. *EMBO J.* **21**, 181–193 (2002).
- McClelland, M.L. *et al.* The highly conserved Ndc80 complex is required for kinetochore assembly, chromosome congression, and spindle checkpoint activity. *Genes Dev.* **17**, 101–114 (2003).
- Li, Y. *et al.* The mitotic spindle is required for loading of the DASH complex onto the kinetochore. *Genes Dev.* **16**, 183–197 (2002).
- Tirnauer, J.S., Grego, S., Salmon, E.D. & Mitchison, T.J. EB1-microtubule interactions in *Xenopus* egg extracts: role of EB1 in microtubule stabilization and mechanisms of targeting to microtubules. *Mol. Biol. Cell* **13**, 3614–3626 (2002).
- Wei, R.R., Sorger, P.K. & Harrison, S.C. Molecular organization of the Ndc80 complex, an essential kinetochore component. *Proc. Natl. Acad. Sci. USA* **102**, 5363–5367 (2005).
- Gillett, E.S., Espelin, C.W. & Sorger, P.K. Spindle checkpoint proteins and chromosome-microtubule attachment in budding yeast. *J. Cell Biol.* **164**, 535–546 (2004).
- Ciferri, C. *et al.* Architecture of the human ndc80-hec1 complex, a critical constituent of the outer kinetochore. *J. Biol. Chem.* **280**, 29088–29095 (2005).
- Wei, R.R. *et al.* Structure of a central component of the yeast dinetochore: rhe Spc24p/Spc25p globular domain. *Structure* **14**, 1003–1009 (2006).
- Hayashi, I. & Ikura, M. Crystal structure of the amino-terminal microtubule-binding domain of end-binding protein 1 (EB1). *J. Biol. Chem.* **278**, 36430–36434 (2003).
- Holm, L. & Sander, C. Protein structure comparison by alignment of distance matrices. *J. Mol. Biol.* **233**, 123–138 (1993).
- Goldsmith, S.C. *et al.* The structure of an actin-crosslinking domain from human fimbrin. *Nat. Struct. Biol.* **4**, 708–712 (1997).
- Gimona, M., Djinnovic-Carugo, K., Kranewitter, W.J. & Winder, S.J. Functional plasticity of CH domains. *FEBS Lett.* **513**, 98–106 (2002).
- Matsudaira, P. Modular organization of actin crosslinking proteins. *Trends Biochem. Sci.* **16**, 87–92 (1991).
- Klein, M.G. *et al.* Structure of the actin crosslinking core of fimbrin. *Structure* **12**, 999–1013 (2004).
- Borrego-Diaz, E. *et al.* Crystal structure of the actin-binding domain of [alpha]-actinin 1: Evaluating two competing actin-binding models. *J. Struct. Biol.* **155**, 230–238 (2006).
- Tirnauer, J.S. & Bierer, B.E. EB1 proteins regulate microtubule dynamics, cell polarity, and chromosome stability. *J. Cell Biol.* **149**, 761–766 (2000).
- Slep, K.C. *et al.* Structural determinants for EB1-mediated recruitment of APC and spectraplakins to the microtubule plus end. *J. Cell Biol.* **168**, 587–598 (2005).
- Tanaka, T.U. *et al.* Evidence that the Ipl1-Sli15 (Aurora kinase-INCENP) complex promotes chromosome bi-orientation by altering kinetochore-spindle pole connections. *Cell* **108**, 317–329 (2002).
- Lampson, M.A., Renduchitala, K., Khodjakov, A. & Kapoor, T.M. Correcting improper chromosome-spindle attachments during cell division. *Nat. Cell Biol.* **6**, 232–237 (2004).
- Cheeseman, I.M. *et al.* Phospho-regulation of kinetochore-microtubule attachments by the Aurora kinase Ipl1p. *Cell* **111**, 163–172 (2002).
- Nousiainen, M., Sillje, H.H.W., Sauer, G., Nigg, E.A. & Korner, R. Phosphoproteome analysis of the human mitotic spindle. *Proc. Natl. Acad. Sci. USA* **103**, 5391–5396 (2006).
- DeLuca, J.G. *et al.* Kinetochore microtubule dynamics and attachment stability are regulated by Hec1. *Cell* **127**, 969–982 (2006).
- Cheeseman, I.M. *et al.* The conserved KMN network constitutes the core microtubule-binding site of the kinetochore. *Cell* **127**, 987–997 (2006).
- Tanaka, K. *et al.* Molecular mechanisms of kinetochore capture by spindle microtubules. *Nature* **434**, 987–994 (2005).
- Miranda, J.J., De Wulf, P., Sorger, P. & Harrison, S.C. The yeast DASH complex forms closed rings on microtubules. *Nat. Struct. Mol. Biol.* **12**, 138–143 (2005).

41. Westermann, S. *et al.* Formation of a dynamic kinetochore-microtubule interface through assembly of the Dam1 ring complex. *Mol. Cell* **17**, 277–290 (2005).
42. Otwinowski, Z. & Minor, W. Processing of X-ray diffraction data collected in oscillation mode. *Methods Enzymol.* **276**, 307–326 (1997).
43. Terwilliger, T.C. & Berendzen, J. Automated MAD and MIR structure solution. *Acta Crystallograph. D Biol. Crystallogr.* **55**, 849–861 (1999).
44. Terwilliger, T. Maximum-likelihood density modification. *Acta Crystallograph. D Biol. Crystallogr.* **56**, 965–972 (2000).
45. Jones, T.A., Zou, J.Y., Cowan, S.W. & Kjeldgaard, M. Improved methods for building protein models in electron density maps and the location of errors in these models. *Acta Crystallogr. A* **47**, 110–119 (1991).
46. Emsley, P. & Cowtan, K. Coot: model-building tools for molecular graphics. *Acta Crystallogr. D Biol. Crystallogr.* **60**, 2126–2132 (2004).
47. Murshudov, G.N., Vagin, A.A. & Dodson, E.J. Refinement of macromolecular structures by the maximum-likelihood method. *Acta Crystallogr. D Biol. Crystallogr.* **53**, 240–255 (1997).
48. Roger, B., Al-Bassam, J., Dehmelt, L., Milligan, R.A. & Halpain, S. MAP2c, but not Tau, binds and bundles F-actin via its microtubule binding domain. *Curr. Biol.* **14**, 363–371 (2004).
49. Honig, B. & Nicholls, A. Classical electrostatics in biology and chemistry. *Science* **268**, 1144–1149 (1995).
50. Chenna, R. *et al.* Multiple sequence alignment with the Clustal series of programs. *Nucleic Acids Res.* **31**, 3497–3500 (2003).